Reexamination of Chlorophyllase Function Implies Its Involvement in Defense against Chewing Herbivores[1][OPEN]

Xueyun Hu, Satoru Makita, Silvia Schelbert, Shinsuke Sano, Masanori Ochiai, Tohru Tsuchiya, Shigeaki F. Hasegawa, Stefan Hörtensteiner, Ayumi Tanaka, and Ryouichi Tanaka*

Institute of Low Temperature Science, Hokkaido University, Sapporo 060–0819, Japan (X.H., M.O., S.F.H., A.T., R.T.); Odawara Research Center, Nippon Soda Co., Ltd., Odawara 250–0280, Japan (S.M., S.Sa.); Institute of Plant Biology, University of Zurich, CH–8008 Zurich, Switzerland (S.Sc., S.H.); Graduate School of Global Environmental Studies (T.T.) and Graduate School of Human and Environmental Studies (T.T.), Kyoto University, Kyoto 606–8501, Japan; and Japan Core Research for Evolutionary Science and Technology, Japan Science Technology Agency, Sapporo 060–0819, Japan (A.T., R.T.)

ORCID IDs: 0000-0002-0022-347X (M.O.); 0000-0002-5858-5326 (R.T.).

Chlorophyllase (CLH) is a common plant enzyme that catalyzes the hydrolysis of chlorophyll to form chlorophyllide, a more hydrophilic derivative. For more than a century, the biological role of CLH has been controversial, although this enzyme has been often considered to catalyze chlorophyll catabolism during stress-induced chlorophyll breakdown. In this study, we found that the absence of CLH does not affect chlorophyll breakdown in intact leaf tissue in the absence or the presence of methyl-jasmonate, which is known to enhance stress-induced chlorophyll breakdown. Fractionation of cellular membranes shows that Arabidopsis (*Arabidopsis thaliana*) CLH is located in the endoplasmic reticulum and the tonoplast of intact plant cells. These results indicate that CLH is not involved in endogenous chlorophyll catabolism. Instead, we found that CLH promotes chlorophyllide formation upon disruption of leaf cells, or when it is artificially mistargeted to the chloroplast. These results indicate that CLH is responsible for chlorophyllide formation after the collapse of cells, which led us to hypothesize that chlorophyllide formation might be a process of defense against chewing herbivores. We found that Arabidopsis leaves with genetically enhanced CLH activity exhibit toxicity when fed to *Spodoptera litura* larvae, an insect herbivore. In addition, purified chlorophyllide partially suppresses the growth of the larvae. Taken together, these results support the presence of a unique binary defense system against insect herbivores involving chlorophyll and CLH. Potential mechanisms of chlorophyllide action for defense are discussed.

Plants have evolved both constitutive and inducible defense mechanisms against herbivores. Constitutive mechanisms include structural defenses (e.g. spines and trichomes) and specific chemical compounds. Constitutive defense mechanisms provide immediate protection against herbivore attacks, although they represent an energy investment by the plant regardless of whether herbivory occurs or not (Mauricio, 1998; Bekaert et al., 2012). By contrast, inducible defense mechanisms do not require an up-front energy cost, although such mechanisms may not be as immediate as constitutive ones when herbivore feeding occurs (Windram et al., 2012). Accordingly, plants exhibit both constitutive and inducible defense mechanisms against herbivory to balance the speed and cost of response. In this regard, it is plausible that the recruitment of abundant primary metabolites for defensive purposes might represent a substantial benefit to plants, providing both a swift and economical defense function.

Toxic chemical compounds form an essential part in both constitutive and inducible defense mechanisms. However, these compounds are potentially a double-edged sword for plants, in a sense that they might pose toxic effects for both plants and herbivores. Plants have evolved an intricate binary system that prevents auto-intoxication by their own chemical compounds. Specifically, a toxic substance is stored in its inactive form and is spatially isolated from specific activating enzymes. These enzymes activate the substance when cells are disrupted by chewing herbivores (Saunders and Conn, 1978; Thayer and Conn, 1981; Morant et al., 2008). One of the most extensively studied binary defense systems is the glucosinolate/myrosinase system, in which the glucosinolate substrate and their hydrolyzing enzyme, a thioglucosidase myrosinase, are compartmentalized. Upon tissue damage, both the substrate and the enzyme
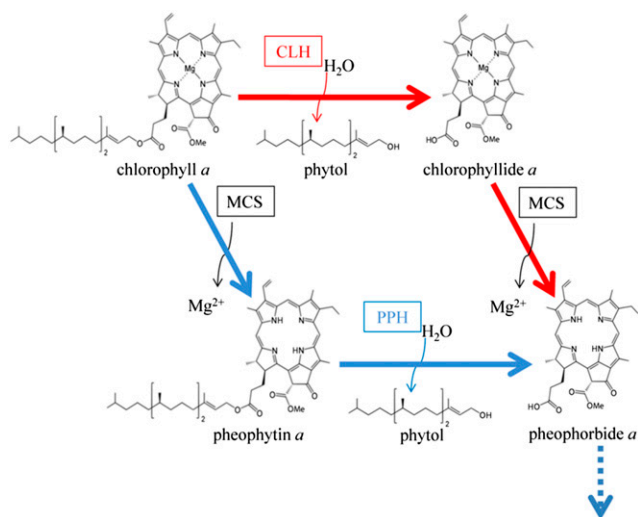
Figure 1. Early steps of proposed chlorophyll breakdown pathways. MCS, Magnesium-dechelating substance.

come into contact to produce unstable aglycones, and various toxic compounds are then spontaneously produced (Bones and Rossiter, 1996). Another well-known example of the binary system is comprised of cyanogenic glucosides and β-glucosidase (Vetter, 2000; Mithöfer and Boland, 2012). In this system, nontoxic cyanogenic glycoside compounds are stored in the vacuole, whereas, the related glycosidase is localized in the cytoplasm. Upon cell destruction by chewing herbivores, the cyanogenic glycosides are hydrolyzed by glycosidase to yield unstable cyanohydrin that is either spontaneously or enzymatically converted into toxic hydrogen cyanide and a ketone or an aldehyde. Because the binary defense system is efficient and effective, a use of ubiquitous compounds for such systems would provide further benefits for plants.

Tetrapyrrole compounds, in particular heme and chlorophyll, are abundant in plant cells. Despite their significant roles in various biological processes including photosynthesis and respiration, many tetrapyrroles are highly toxic to plant and animal cells, if present in excess amounts (Kruse et al., 1995; Meskauskiene et al., 2001). Their photodynamic properties can cause the generation of reactive oxygen species upon illumination, resulting in cell injury or direct cell death. For example, Tapper et al. (1975) showed that a tetrapyrrole compound (pheophorbide a), which is readily converted from dietary chlorophyll through the loss of magnesium and phytol, reduces the growth and survival rates of young albino rats through its photodynamic property. More recently, Jonker et al. (2002) demonstrated that dietary-derived pheophorbide a causes severe damages
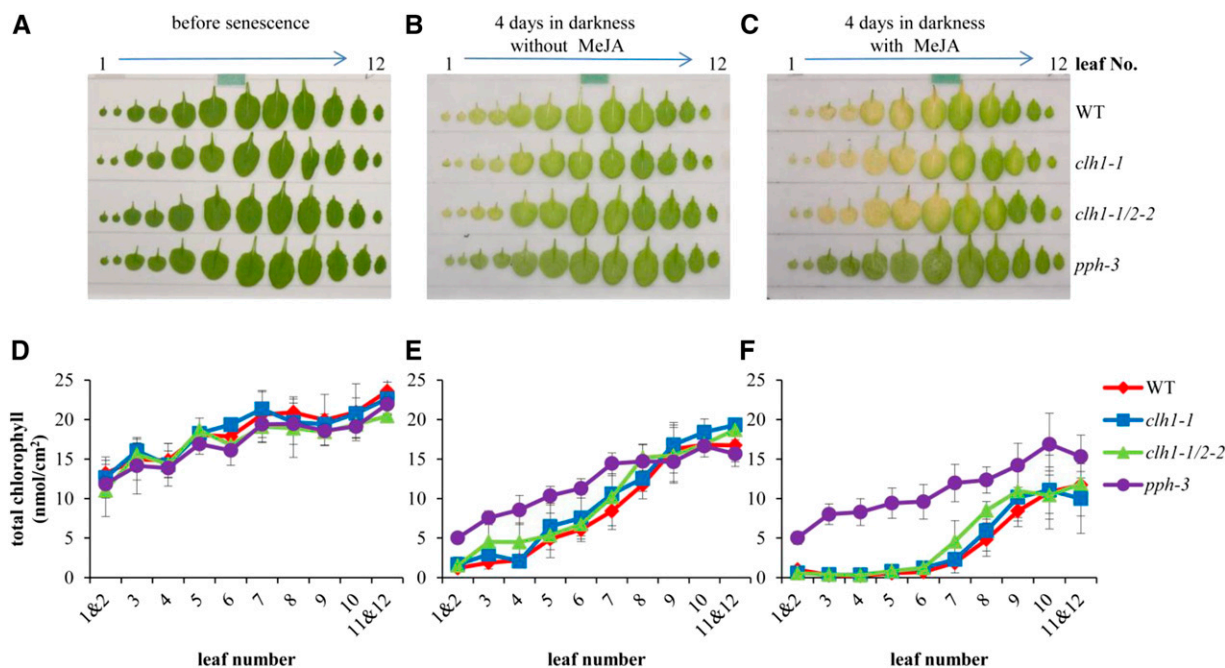

Figure 2. MeJA promotes chlorophyll degradation in the *clh* mutants as well as in the wild type (WT). Chlorophyll degradation in leaves of Arabidopsis wild-type, *clh1-1*, *clh1-1/clh2-2*, and *pph-3* plants after 4 d of dark-induced leaf senescence in the absence (B and E) or presence (C and F) of 50 μM MeJA, compared with chlorophyll levels in leaves prior to the induction of leaf senescence (A and D). Leaf images are shown at top (A–C), and chlorophyll levels of the corresponding leaves are shown at bottom (D–F). Leaf numbers are counted from the bottom (oldest) to top (youngest) of the plant. For chlorophyll measurement, the oldest leaves (nos. 11 and 12) and the youngest leaves (nos. 1 and 2) were pooled prior to chlorophyll extraction. Data represent the mean ± SD of three biological replicates.

on the skin of mutant mice that lack a transporter to excrete pheophorbide *a* from cells. These studies indicate that incorporation of an excessive amount of tetrapyrrole compounds can induce photosensitization in animals. Previous studies also showed that tetrapyrroles have illumination-independent deleterious effects on insects. For example, pheophorbide *a* affected the assimilation of the plant sterols to synthesize developmental hormones of insects by inhibiting the activity of a key enzyme, cholesterol acyltransferase (Song et al., 2002). Moreover, some tetrapyrroles, including pheophorbide *a*, have been suggested to induce illumination-independent cell death in plants as well by an unknown

mechanism (Hirashima et al., 2009). It is proposed that organisms use the toxicity of tetrapyrroles for their defense systems. The larvae of tortoise beetle (*Chelymorpha alternans*) even utilize pheophorbide *a* as a powerful deterrent in the fecal shield to protect themselves from their predators (Vencl et al., 2009). Kariola et al. (2005) suggested that a chlorophyll derivative, chlorophyllide, is involved in the defense against fungi, based on their observations that down-regulation of a chlorophyll-hydrolyzing enzyme, chlorophyllase (CLH), results in increased susceptibility of Arabidopsis (*Arabidopsis thaliana*) plants to the necrotrophic fungus *Alternaria brassicicola*.
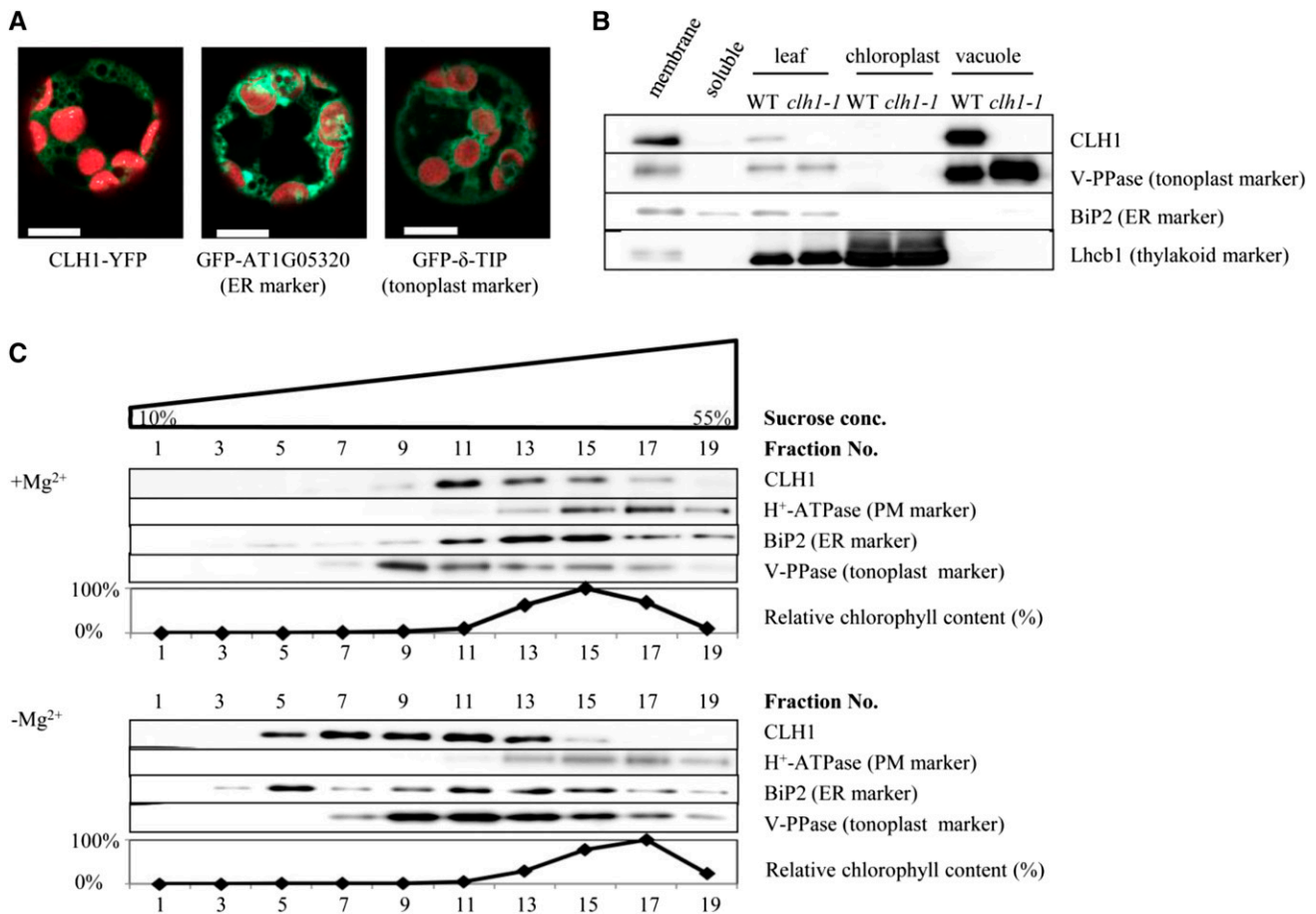

Figure 3. Subcellular localization of Arabidopsis CLH1. A, CLH1-yellow fluorescent protein (YFP) fusion protein (green) was detected outside of chloroplasts (red) in leaf protoplasts prepared from plants constitutively expressing CLH1-YFP (left). For comparison, protoplasts were prepared from transgenic plants expressing GFP-AT1G05320 (ER marker, middle) or GFP-δ-tonoplast intrinsic protein (TIP; tonoplast marker, right). B, Leaf tissue was fractionated into membrane, soluble, intact chloroplast, and vacuole fractions for the analysis of CLH1 localization as described in "Materials and Methods." Total leaf, chloroplast, and vacuole fractions were prepared from both the wild type (WT) and the *clh1* mutant, and the membrane and soluble fractions were prepared from the wild type only. From membrane/soluble, leaf, chloroplast, and vacuolar samples, 2, 12, 12, and 4 μg of protein, respectively, were loaded on an SDS-PAGE gel. The blotted membrane was then immunologically detected with anti-CLH1, anti-V-PPase, anti-lumenal-binding protein2 (BiP2), and anti-LHCII type I chlorophyll *a/b*-binding protein (Lhcb1) antisera. C, Cellular membranes were separated into 20 fractions by Suc density gradient centrifugation of microsomal fractions in the presence (+Mg^{2+}) or absence of Mg^{2+} (–Mg^{2+}). Odd-numbered fractions were analyzed by immunoblotting with anti-CLH1, anti-H$^+$-ATPase, anti-BiP2, and anti-V-PPase antibodies. Thylakoid membrane concentrations are represented by relative chlorophyll contents in each fraction. PM, Plasma membrane. Bars = 10 μm.
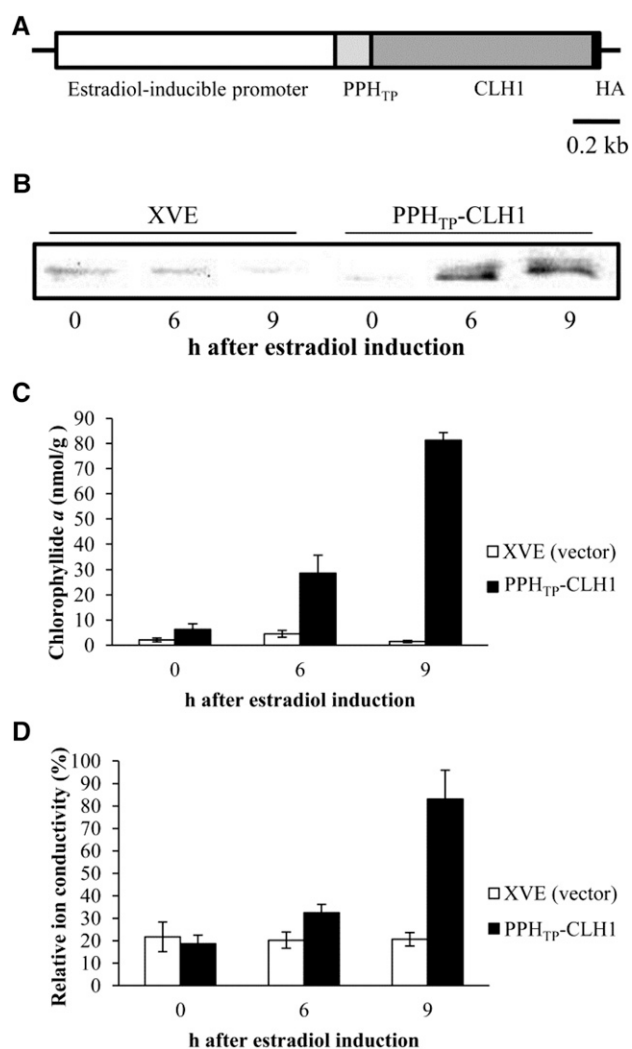
Figure 4. Mistargeting of CLH1 to chloroplasts. A, The PPH_{TP}-CLH1 construct is composed of an estradiol-inducible promoter, the 5' end of *PPH* encoding the chloroplast transit peptide (PPH_{TP}), the full-length cDNA of *CLH1* without its start codon, and a human influenza hemagglutinin (HA)-tag B to D, Leaves of Arabidopsis lines harboring either the activator unit only as control (XVE, which denotes the DNA-binding domain of the bacterial repressor LexA [X], the acidic transactivating domain of VP16 [V], and the carboxyl region of the human estrogen receptor [E]) or both the activator and the responder unit (PPH_{TP}-CLH1) were treated with estradiol for the indicated times in the dark. B, Immunoblot analysis of CLH1 protein in the XVE- and PPH_{TP}-CLH1-expressing leaves. Note that the top signal also seen in XVE is unspecific. C, Accumulation of chlorophyllide *a* after induction of chloroplast-localizing CLH1. Data are mean ± sd of three biological replicates. D, Ion leakage as a measure for cell death after reexposure to light of estradiol-treated leaves for 2 h. Data are mean ± sd of six biological replicates.

In this study, we examined the possibility that plants use tetrapyrroles for defense against herbivores by analyzing CLH, a well-known hydrolase common in plants. Chlorophyll consists of a tetrapyrrolic macrocycle and a hydrophobic phytol side chain (Fig. 1). Phytol hydrolysis results in the formation of chlorophyllide (Fig. 1), a less hydrophobic chlorophyll

derivative, which has photochemical properties similar to chlorophyll. Two different plant enzymes are known to catalyze the cleavage of phytol, pheophytinase (PPH) and CLH. PPH is a chloroplast-located enzyme that specifically catalyzes the removal of phytol from Mg-free chlorophyll catabolites (Schelbert et al., 2009). This enzyme was only recently discovered and has been shown to be responsible for chlorophyll degradation during leaf senescence. By contrast, CLH has a broader substrate specificity and removes the side chain from chlorophyll or other chlorophyll derivatives (McFeeters et al., 1971). CLH activity was first reported in leaf extracts in 1913 (Willstätter and Stoll, 1913), but despite a century of research, in vivo function and intracellular localization of this enzyme remained controversial. Some reports have indicated CLH to localize to chloroplasts (Azoulay Shemer et al., 2008; Azoulay-Shemer et al., 2011), while Schenk et al. (2007), by examining the intracellular localization of transiently expressed CLH-GFP fusions, proposed Arabidopsis CLH to localize outside the chloroplast. Schenk et al. (2007) also reported that the lack of CLH does not affect chlorophyll degradation during leaf senescence. However, it remains possible that CLH is specifically involved in chlorophyll degradation in response to stresses that activate jasmonate signaling, such as wounding or pathogen attack. This hypothesis is based on the observation that the expression of a *CLH* gene was highest when methyl-jasmonate (MeJA; a derivative of jasmonic acid) was applied to Arabidopsis plants (Tsuchiya et al., 1999).

Here, we report that CLH is not involved in endogenous chlorophyll breakdown even when leaf senescence was promoted by jasmonate signaling. CLH is shown to localize to the chlorophyll-free endoplasmic reticulum (ER) and the tonoplast of intact plant cells. We found that CLH promotes the conversion of chlorophyll into chlorophyllide when leaf cells are disrupted or when CLH is genetically mislocalized to chloroplasts. To examine the possibility that plants use chlorophyll and CLH to form a binary defense system against herbivores, a generalist herbivore, *Spodoptera litura* larvae, was employed to investigate the toxicity of Arabidopsis leaves with genetically enhanced CLH activity and purified chlorophyllide. The results support our hypothesis, indicating plants to deploy an abundant photosynthetic pigment for defense against herbivores, which would be economic and provide adaptation benefits to plants. A potential mechanism of chlorophyllide action as part of the plant defense system is discussed based on the examination of chlorophyllide binding to the insect gut.

RESULTS

CLH Is Not Involved in MeJA-Promoted Chlorophyll Degradation

To better understand the biological role of CLH, we first determined whether CLH is required for chlorophyll breakdown that occurs under MeJA-induced stress conditions. Although the genome of Arabidopsis

encodes two isoforms of CLH, CLH1 (AT1G19670.1) and CLH2 (AT5G43860.1), CLH1 represents the majority of detectable CLH activity in Arabidopsis (Supplemental Fig. S1A; Schenk et al., 2007). Wild-type and mutant Arabidopsis plants that lack CLH1 or both isoforms of CLH were treated with MeJA in the dark. The CLH1 protein was present before plants were transferred to darkness, and CLH1 levels increased within the first 4 d in the dark and later decreased again (Supplemental Fig. S1B). MeJA treatment enhanced the CLH1 protein level at the second and fourth day in the dark (Supplemental Fig. S1B). However, despite the increased CLH levels in MeJA-treated plants, chlorophyll breakdown was indistinguishable between wild-type, *clh1*, and *clh1/clh2* mutant plants (Fig. 2). By contrast, chlorophyll degradation was significantly delayed in an Arabidopsis mutant that lacks PPH, known to be associated with chlorophyll catabolism (Schelbert et al., 2009). These data indicate that PPH, not CLH, is responsible for the majority of MeJA-enhanced chlorophyll breakdown, even though CLH1 is highly induced by MeJA.

CLH1 Is Localized to the Tonoplast and the ER

The intracellular localization of CLH1 was analyzed in transgenic Arabidopsis plants constitutively expressing a fusion of CLH1 with YFP. Our observations indicate that the YFP signal was localized outside of chloroplasts that emitted red chlorophyll autofluorescence but was located in vesicular structures that resemble the ER or the tonoplast (Fig. 3A). The membrane and tonoplast localization of native CLH1 was subsequently confirmed by subcellular fractionation in wild-type Arabidopsis plants using an anti-CLH1 antiserum (Fig. 3B). Cellular membrane fractions were further fractionated by Suc density

gradient centrifugation and analyzed for the localization of CLH1 (Fig. 3C). During Suc density gradient centrifugation, rough ER membranes aggregate in the presence of Mg^{2+}, causing migration to heavier density portions in the gradient (Oka et al., 2010; Wulfetange et al., 2011). CLH1 distribution shifted from lighter portions (fractions 5–13) in the absence of Mg^{2+} to heavier portions (fractions 11–17) of the Suc gradient in the presence of Mg^{2+}. The distribution of the ER marker (BiP2 protein) showed two peaks (fractions 5 and 13; Fig. 3C) in the absence of Mg^{2+}, but the lighter peak appeared to shift to heavier portions of the Suc gradient in the presence of Mg^{2+}. This shift appears to correlate with the localization of CLH1 (Fig. 3C). Additionally, CLH1 distribution partly overlapped with that of a tonoplast marker, pyrophosphate-energized vacuolar membrane proton pump1 (V-PPase; Fig. 3C). By contrast, the distribution of chlorophyll or a plasma membrane marker (plasma membrane proton-translocating adenosine triphosphatase [H^+-ATPase]) was distinct from CLH1 (Fig. 3C). MeJA treatment of leaves did not change CLH1 distribution in the Suc gradient fractions (Supplemental Fig. S2). Taken together, these data indicate that CLH1 is localized at the ER and the tonoplast.

Chlorophyllide Is Formed Only When CLH and Chlorophyll Are Forced to Contact Each Other

Based on these results, we hypothesized that CLH1 is involved in defense responses and that it catalyzes chlorophyllide formation upon cell disruption, a mechanism that might be similar to binary defense systems in which an enzyme (such as β-glucosidase) locating in a certain cellular compartment activates a chemical defense compound (such as cyanogenic glycosides) stored in another compartment upon cell disintegration by
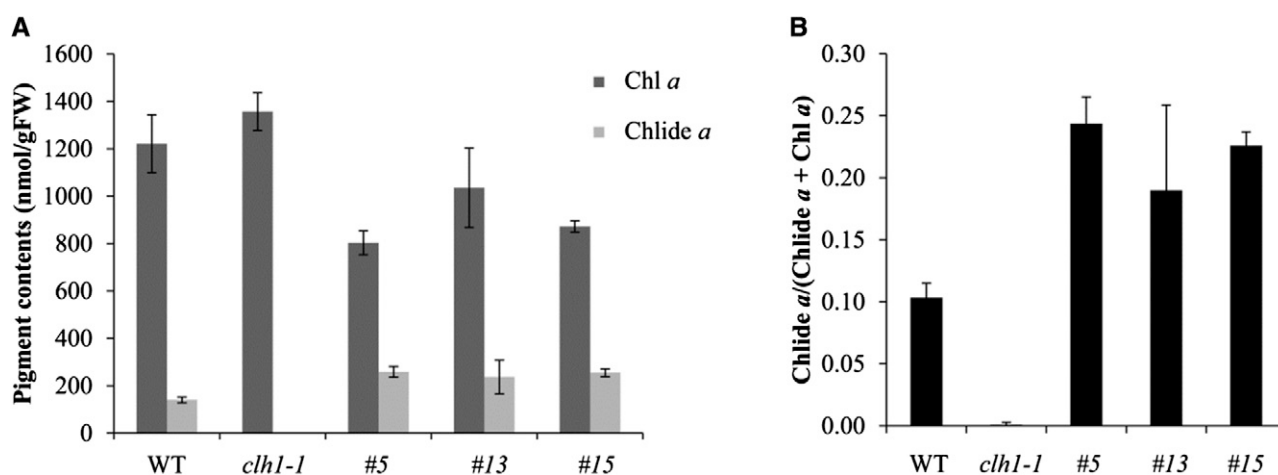
Figure 5. Chlorophyllide formation after mechanical disintegration of leaves. The leaves of the Arabidopsis wild type (WT), *clh1-1*, and three independent transgenic lines overexpressing CLH1-YFP (nos. 5, 13, and 15) were disrupted as it was described in "Materials and Methods." A, Chlorophyll *a* (Chl *a*) and chlorophyllide *a* (Chlide *a*) contents in leaf homogenates. B, Values are given as the ratio of Chlide *a* to Chl *a* + Chlide *a*. Data points represent the mean ± SD of five biological replicates. FW, Fresh weight.

herbivores (Vetter, 2000; Mithöfer and Boland, 2012). To verify the hypothesis that spatial contact between CLH1 and thylakoid-embedded chlorophyll in the same organelle is sufficient to induce chlorophyllide formation, transgenic wild-type plants were produced that mistarget CLH1 to chloroplasts after estradiol induction. Induction of chloroplast-localizing CLH1 rapidly caused formation of chlorophyllide and resulted in the death of the induced tissue upon illumination (Fig. 4; Supplemental Fig. S3).

Subsequently, chlorophyllide formation was analyzed after mechanical disruption of cellular integrity of leaves to determine if CLH actively produces chlorophyllide under conditions that mimic cell disruption by herbivores. Sixty minutes after wild-type leaf disruption, a substantial portion of chlorophyll (10% of total chlorophyll) was converted to chlorophyllide, while chlorophyllide formation was further increased to nearly 25% of the total chlorophyll level in leaves of three independent CLH1-YFP-overexpressing lines but was almost absent in *clh1-1* (Fig. 5). These results imply that large amounts of chlorophyllide could be produced by CLH1 when cells are disrupted by leaf-chewing herbivores.

Leaves with Genetically Enhanced CLH Activity Exhibit Toxicity to *S. litura* Larvae

To examine the possible contribution of CLH1 to herbivory defense mechanisms, leaves from wild-type, *clh1-1*, and CLH1-YFP-overexpressing plants were fed to *S. litura* larvae, a generalist insect that feeds on a wide range of plants. Five freshly hatched larvae were fed on single plants of each line for 11 d. Severely eaten plants were replaced by fresh ones every 2 or 3 d (Supplemental Fig. S4). Approximately 10% of larvae that were fed leaves from the overexpressing plants were dead after 11 d of feeding, while nearly all larvae fed on wild-type or *clh1-1* leaves survived (Fig. 6A). These results indicate that the increased CLH1 activity in transgenic plants (Fig. 5) caused a toxic effect on larvae. Apparently, CLH1 activity in the wild type was not high enough to kill larvae.

Purified Chlorophyllide Shows Toxicity to *S. litura* Larvae

To assess whether the effect of CLH1 overexpression on larval survival was due to chlorophyllide formation, purified chlorophyll, chlorophyllide, or pheophorbide, a Mg-free derivative of chlorophyllide known to be toxic to animals (Tapper et al., 1975; Jonker et al., 2002) was administered to a total of about 200 *S. litura* larvae for 11 d by mixing the compounds with a commercially available artificial diet (Fig. 6B; Supplemental Table S1; Supplemental Fig. S5). The larvae were divided into five groups, and each group of larvae was administered with artificial diet containing only solvent (0.1% [w/w] dimethylformamide), 400 nmol g^{-1} chlorophyll, 200 nmol g^{-1} chlorophyllide, 400 nmol g^{-1} chlorophyllide, or 400 nmol g^{-1} pheophorbide, respectively. Wild-type
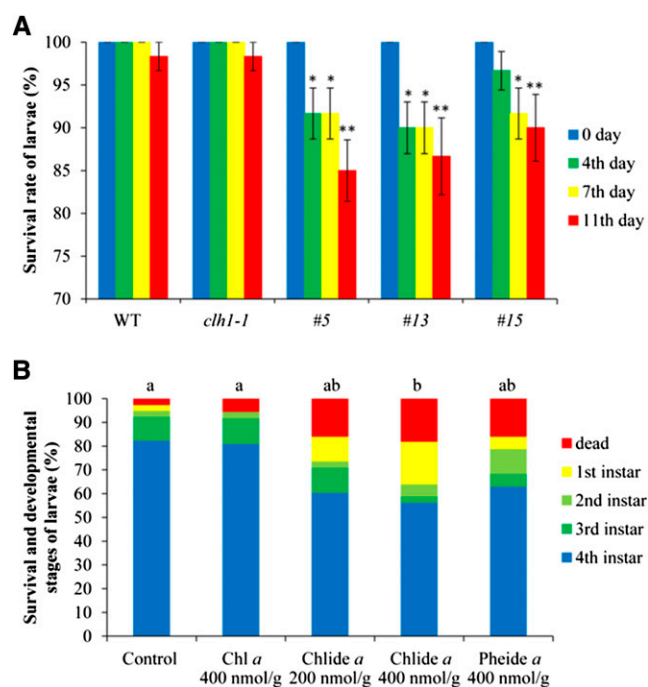

Figure 6. CLH-overexpressing leaves and purified chlorophyllide show toxicity to *S. litura* larvae. A, Survival rates of *S. litura* larvae fed for up to 11 d with Arabidopsis leaves from the wild type (WT), *clh1-1*, and three CLH1-YFP-overexpressing lines. Single and double asterisks indicate significant differences (*$P < 0.05$ and **$P < 0.01$) detected by the χ^2 test between each line within the same duration of feeding. Error bars represent SE of the mean for 12 biological replicates, with each replicate including five larvae. B, Groups of 35 to 40 freshly hatched *S. litura* larvae were fed for 11 d with an artificial diet mixed with purified pigments at the indicated final concentrations. The Kruskal-Wallis test indicated that the developmental stages of the larvae were significantly ($P < 0.05$) different among treatments. Each pair of treatments was then statistically assessed by the pairwise Wilcoxon rank sum test with each developmental stage as an ordinal variable as described in "Materials and Methods." Treatments that are not statistically different ($P < 0.05$) are indicated with the same alphabetical letters (a or b). The calculated P values are shown in Supplemental Table S2. Chl *a*, Chlorophyll *a*; Chlide *a*, chlorophyllide *a*; Pheide *a*, pheophorbide *a*.

Arabidopsis leaves contain approximately 2 μmol chlorophyll g^{-1} fresh weight, and thus the administrated pigment concentrations corresponded to 10% to 20% of leaf chlorophyll content. Administration of the photosynthetic pigments significantly affected the survival and growth of larvae, as the differences between treatments were detected with the Kruskal-Wallis test ($P < 0.01$). Administration of chlorophyll did not impact the survival rates of larvae, while both chlorophyllide and pheophorbide slightly reduced the survival rate of larvae. Analysis with a Fisher's exact test confirmed a marginally significant difference in the survival rates between treatments ($P = 0.085$). Administration of chlorophyll-containing diet allowed 80% of the larvae to develop to the fourth instar (Fig. 6B). By contrast, larval development was significantly reduced by administration of 400 nmol g^{-1} chlorophyllide *a* (Fig. 6B; Supplemental

Table S2). Specifically, only 60% of the larvae reached the fourth instar, while approximately 20% of the larvae were killed and an increased population remained in the first or second instar with this treatment. These results indicate that both chlorophyllide and pheophorbide exert toxic effects on larvae, although the toxicity of pheophorbide was only marginally significant in our experiments.

Chlorophyllide Is Preferentially Bound to the Midgut of Silkworm

The mechanism(s) of how chlorophyllide exerts toxicity to *S. litura* larvae is not clear at this stage. A possibility is that chlorophyllide interacts with certain proteins to inhibit their functions in the larval gut. To explore this possibility, we examined pigment compositions in larval midguts. For this purpose, silkworm (*Bombyx mori*) larvae were used instead of *S. litura*, because the size of *S. litura* larvae is too small to technically allow the analysis of pigments in their midguts. Accordingly, we fed leaves of mulberry (*Morus alba*) instead of Arabidopsis, because silkworms only feed on mulberry leaves. To examine the effect of CLH activity on pigment binding to the insect gut, we reared silkworm larvae for 26 d by feeding fresh mulberry leaves. After 26 d of feeding, larvae (on the fourth day of their fifth instar) were sacrificed to determine pigment composition in the midgut contents (partially digested food remained in the midgut), midgut tissue, and frass (Fig.

7). HPLC profiles showed that the chlorophyllide *a* (peak 2) contents were significantly lower than those of chlorophyll *a* (peak 7) in the midgut contents and frass. By contrast, chlorophyllide *a* contents in the midgut tissue were predominantly higher than those of chlorophyll *a* in the same tissue. The chlorophyllide *a* to chlorophyll *a* ratio in midgut tissue was approximately 8, while it was less than 0.05 in both midgut contents and frass (Fig. 7B). These results indicate that the midgut preferentially binds chlorophyllide.

DISCUSSION

We have demonstrated here that the major isoform of CLH, CLH1, is localized in the tonoplast and the ER (Fig. 3). When cellular membrane structures are disintegrated, CLH comes into contact with chlorophyll and converts it to chlorophyllide (Fig. 5). Arabidopsis leaves with genetically enhanced CLH activity as well as purified chlorophyllide shows toxicity toward the generalist herbivore *S. litura* (Fig. 6), implying that CLH and chlorophyll form a binary defense system against herbivores.

Tonoplast and ER localization of CLH1 in intact cells spatially segregates CLH1 from its substrate, chlorophyll. Other plant defense compounds, such as phenolic compounds (War et al., 2012) or glucosinolates (Saunders and Conn, 1978; Bones and Rossiter, 1996; Morant et al., 2008; War et al., 2012), are also compartmentalized distinct from the enzymes that activate
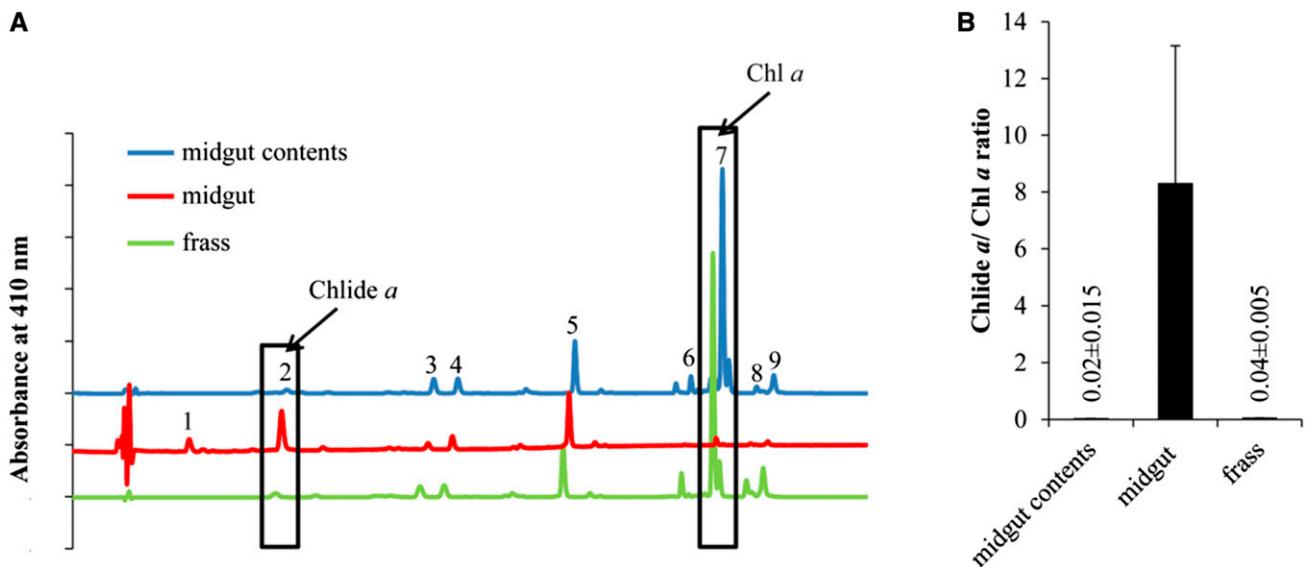

Figure 7. Different compositions of photosynthetic pigments in the midgut contents (food remained inside of the midgut), midgut tissue, and frass of 26-d-old silkworm larvae. A, HPLC chromatograms for photosynthetic pigments extracted from midgut contents, midgut tissue, and frass of 26-d-old silkworm larvae, respectively. Peak 1, Chlorophyllide *b*; peak 2, chlorophyllide *a*; peak 3, neoxanthin; peak 4, violaxanthin; peak 5, lutein; peak 6, Chlorophyll *b*; peak 7, Chlorophyll *a*; peak 8, pheophytin *a*; peak 9, β-carotene. The scales of chromatograms were normalized with the heights of the lutein peaks. Black rectangle boxes were used to emphasize the relative contents of chlorophyllide *a* and chlorophyll *a* in the different samples. B, Chlorophyllide *a* to chlorophyll *a* ratio in the midgut contents, midgut tissue, and frass of 26-d-old silkworm larvae. Data points represent the mean ± SD of three biological replicates. Chl *a*, Chlorophyll *a*; Chlide *a*, chlorophyllide *a*.

them. With regard to herbivory, such a binary defense system appears to be a common strategy in plants that prevents uncontrolled activation of toxic compounds, but enables their instant activation upon attack of chewing insect herbivores. Furthermore, utilizing a ubiquitous photosynthetic pigment for defense is cost efficient and may confer a selective advantage.

This and previous studies (Hu et al., 2013) show that disruption of plant cells renders chlorophyll accessible to CLH, which immediately begins to hydrolyze the pigment into chlorophyllide. Because chlorophyll hydrolysis is known to occur commonly in the gut of insect herbivores (Park et al., 2003; Badgaa et al., 2014), it is plausible that CLH continues to produce chlorophyllide as the ingested leaf tissue passes through the insect guts.

At this time, the precise mechanism regarding how chlorophyllide exerts toxicity for larvae remains unclear. Accordingly, the reason why chlorophyllide is more toxic than chlorophyll is still unknown. If a well-known photodynamic property of tetrapyrrole compounds is taken into consideration, a possible explanation is that chlorophyllide is more efficiently taken up into insect blood than chlorophyll, and chlorophyllide exerts photodynamic effects on larval cells. Alternatively, we speculate that chlorophyllide might bind certain larval gut proteins and/or might inhibit assimilation. This hypothesis is consistent with our observation that the midgut preferentially binds chlorophyllide over chlorophyll. Tetrapyrrole molecules are known to bind a variety of proteins and to inhibit their functions (Miller and Shaklai, 1999; Golovina et al., 2013; Kraatz et al., 2014). For example, pheophorbide a is an inhibitor of the enzyme, cholesterol acyltransferase (Song et al., 2002). Thus, it would be reasonable to assume that a high level of chlorophyllide inhibits certain functions of midgut proteins. However, silkworms were shown to contain red fluorescent proteins, which bind chlorophyllide in the digestive juice and/or midgut tracts (Hayashiya, 1978; Mauchamp et al., 2006; Pandian et al., 2008). It was proposed that these proteins utilize bound chlorophyllide for antibacterial and antiviral activities of the larva (Pandian et al., 2008). Interestingly, tortoise beetle larvae have evolved to utilize pheophorbide a as a deterrent in a fecal shield to protect themselves from their predators (Vencl et al., 2009). A defensive compound could have contrasting effects against different insect species. For example, condensed tannins have antiherbivore activity for some insects, but they could function as nutritive substrates for other insect species (Bernays and Woodhead, 1982). Noteworthy, the Arabidopsis defense system composed of CLH1 and chlorophyll does not seem to be effective enough to completely suppress the growth of *S. litura* larvae (Fig. 6A), supporting the idea that insect herbivores may have counter-developed tolerance against the toxicity of phytol-free chlorophyll derivatives during evolution. We speculate that many insects have evolved to overcome toxicity of ubiquitous defense mechanisms of plants, such as tannins, so that ubiquitous compounds often do not show strong toxicity to insect herbivores (Ayres et al., 1997).

Otherwise, insects could not feed on such a variety of plants.

CLH-encoding genes are ubiquitously distributed in the genomes of land plants; thus, it is reasonable to assume that CLH confers a certain selective advantage. It was shown that jasmonate-insensitive Arabidopsis mutants become susceptible to herbivores or detritivores, such as *Porcellio scaber* and *Armadillidium vulgare*, which usually do not feed on Arabidopsis (Farmer and Dubugnon, 2009; Abe et al., 2013). We speculate that the efficiency of the CLH/chlorophyll defense system may vary between insect species and among different plant species. It will be necessary in the future to investigate the effects of CLH on a wider range of plant species and potential herbivores. Our study implies that plants use CLH and chlorophyll as a unique binary defense system. This will help researchers to exploit potential plant-herbivore interaction through this mechanism in the future.

MATERIALS AND METHODS

Plant Materials and Senescence Induction

The Arabidopsis (*Arabidopsis thaliana*) transfer DNA insertion lines SALK_124978 (designated *clh1-1*; ecotype Columbia [Col-0]), SAIL_646_E09 (designated *clh2-2*; Col-0), and *clh1-1/clh2-2* were described by Schenk et al. (2007). The transfer DNA insertion line GK-453A08 (designated *pph-3*; Col-0), which lacks PPH (Schelbert et al., 2009), was obtained from the European Arabidopsis Stock Center. The GFP::complementary DNA (cDNA) transgenic lines (Q4 [GFP-AT1G05320] and Q5 [GFP-δ-TIP]), which were described by Cutler et al. (2000), were obtained from The Arabidopsis Information Resource. Plants were grown in soil under either long-day (16 h of light/8 h of dark) or short-day (10 h of light/14 h of dark) growth conditions under fluorescent light (70–90 μmol photons m^{-2} s^{-1} at 23°C). To analyze chlorophyll degradation during leaf senescence, Arabidopsis plants were grown under long-day conditions, and all rosette leaves were subsequently detached from plants, placed on wet filter paper moistened with a buffer containing 3 mM MES (pH 5.8) with or without 50 μM MeJA, and incubated in darkness for 4 d.

Chlorophyll Analysis and Pigment Preparation

Leaves were imaged with a digital camera after removal from their parent plant, and leaf area was calculated using ImageJ software (http://rsbweb.nih.gov/ij/). Chlorophyll was extracted from leaf tissue by homogenization with acetone, which was precooled at –30°C (Hu et al., 2013). Extracts were subsequently centrifuged for 5 min at 20,000g at 4°C, and the supernatant was analyzed by HPLC using a symmetry C8 column (150-mm length and 4.6-mm i.d.; Waters) according to the method of Zapata et al. (2000). Pigment concentrations were estimated from the absorption monitored at 410 nm. Standard pigments (chlorophyll a and b) were purchased from Juntec Co., Ltd., and pheophorbide a was purchased from Wako Pure Chemical Industries, Ltd.

For pigment feeding experiments (Fig. 6B), chlorophyll and chlorophyllide were prepared from garland chrysanthemum (*Glebionis coronaria*) purchased from a supermarket in Sapporo, Japan, according to the method of Müller et al. (2011) with slight modifications as follows. Leaves were ground in liquid nitrogen using mortar and pestle, and 5 to 10 g of fine powder was suspended in 20 mL of acetone and 20 mL of 0.2 M Tricine-NaOH (pH 8.0). The mixture was agitated for 2 h at room temperature in the dark, and then leaf debris was removed by centrifugation. The resulting green supernatant was repeatedly extracted with 40 mL of hexane until the hexane phase was colorless. The chlorophyll-containing hexane phases were pooled and dried under N$_2$. Chlorophyllide was extracted from the acetone phase with diethyl ether, and the diethyl ether was dried under N$_2$. Partially purified chlorophyll and chlorophyllide was dissolved in small volumes of pure acetone prior to HPLC purification. Chlorophyllide a was isolated on a preparative column (250-mm length and 20-mm i.d.; Shim-pack Prep-ODS, Shimadzu) using the binary

solvent system developed by Zapata et al. (2000) with solvent A (methanol:acetonitrile:0.25 M aqueous pyridine [50:25:25, v/v/v]) and solvent B (methanol:acetonitrile:acetone [20:60:20, v/v/v]). Chlorophyllide a was eluted at 9 mL min^{-1} using the following gradient of solvent B (v/v) in solvent A: 0 min, 40%; 11 min, 100%; 25 min, 100%; 27 min, 40%; and 30 min, 40%. Chlorophyll a was purified with the same preparative column but with isocratic elution using solvent B. After fractionation of chlorophyll a and chlorophyllide a, these pigments were recovered in diethyl ether, and the solvents were removed by a stream of N_2 gas.

Cloning and Arabidopsis Transformation

A cDNA covering the coding region of *CLH1* (AT1G19670) was cloned from a wild-type Arabidopsis cDNA pool. The YFP DNA sequence was added to the 3′ end of CLH1, and then the 5′ untranslated region (65 bp) and 3′ untranslated region (199 bp) of the *CLH1* gene were fused, respectively, to the 5′ and 3′ end of the fusion sequence. The fused sequences were cloned into pEarleyGate100 (Earley et al., 2006). The construct was introduced into *Agrobacterium tumefaciens* strain GV2260 and used to infect Arabidopsis with the floral dip method (Clough and Bent, 1998). Two-week-old seedlings of transformants were selected by spraying with BASTA. Three independent lines (nos. 5, 13, and 15) were selected for further analysis. Third generation homozygous plants were used for the feeding experiments as described below.

For targeting of CLH1 to chloroplasts, the coding sequence of *CLH1* with an HA-tag added at the 3′ end but without start codon was cloned behind the 5′ end of *PPH* encoding the PPH transit peptide (PPH$_{TP}$; Schelbert et al., 2009) to produce a chimeric protein (PPH$_{TP}$-CLH1) that targets CLH1 to the chloroplast. The construct was recombined into the responder plasmid pMDC221 of a two-component expression system allowing estradiol-inducible expression of genes of interest (Brand et al., 2006). Arabidopsis wild-type plants were transformed in two successive steps, first, with the activator unit pMDC150-35S expressing the chimeric transcription factor XVE under the control of the 35S promoter (Brand et al., 2006). Primary transformants were selected on kanamycin and were propagated to the second generation to be used as controls (labeled XVE in Fig. 4 and Supplemental Fig. S3) or were supertransformed with pMDC221-PPH$_{TP}$-CLH1, which was double selected on kanamycin and hygromycin and propagated to the second generation to produce PPH$_{TP}$-CLH1-expressing plants (labeled PPH$_{TP}$-CLH1 in Fig. 4 and Supplemental Fig. S3).

Confocal Microscopy

Intact protoplasts were isolated from mature leaves of 4-week-old transgenic plants by the method of Robert et al. (2007). The localization of the YFP- or GFP-tagged fusion protein in transgenic plants was observed using confocal fluorescence microscopy (Nikon D-Eclipse C1si confocal microscope) with the excitation wavelength of 488 nm, and emission was collected at 496 to 706 nm.

Preparation of Membrane and Soluble Fractions

Membrane and soluble fractions were prepared from the leaves of 7-week-old plants grown under short-day conditions as described by Oka et al. (2010) with slight modification. Briefly, leaf tissue was homogenized with a solution containing 100 mM MOPS-NaOH (pH 7.0), 1 mM MnCl$_2$, and a protease inhibitor cocktail (Sigma), and the suspension was centrifuged at 4°C for 10 min at 3,000g. Supernatants were subsequently centrifuged at 4°C for 60 min at 160,000g to generate a pellet (membrane) fraction and a supernatant (soluble) fraction.

Isolation of Intact Chloroplasts and Vacuoles

Rosette leaves were harvested from 7-week-old plants grown under short-day conditions. Intact chloroplasts were prepared according to the method of Salvi et al. (2008). Intact vacuoles were prepared according to the protocol of Robert et al. (2007). Samples were stored at –80°C until use.

Membrane Fractionation

Mature leaves from Arabidopsis plants grown in soil for 7 weeks under short-day conditions were used for membrane fractionation in a Suc density gradient. The fractionation method was modified from that described by Oka

et al. (2010) and Wulfetange et al. (2011). Leaves were homogenized in a blender with 10 volumes (v/w) of homogenization buffer containing 50 mM Tris (pH 7.6 at 22°C), 20% (v/v) glycerol, and 150 mM NaCl with either 5 mM MgCl$_2$ and 2 mM EGTA (for subsequent Suc gradient separation in the presence of Mg^{2+}) or with only 2 mM EDTA (for subsequent Suc gradient separation in the absence of Mg^{2+}). The homogenates were filtered through two layers of Miracloth (Merck) and then centrifuged at 4°C for 10 min at 10,000g. The supernatants were subsequently ultracentrifuged at 4°C for 30 min at 100,000g. The resulting pellets containing the microsomal fraction were resuspended in 0.5 mL g^{-1} resuspension buffer containing 50 mM MOPS-NaOH, (pH 7.0), 10% (w/v) Suc, EDTA-free complete protease inhibitor cocktail (Sigma), and either 2 mM EDTA or 5 mM MgCl$_2$. The suspensions were then centrifuged at 4°C for 3 min at 6,000g to remove any unsuspended material. Six hundred microliters of supernatants were loaded onto the top of the following discontinuous Suc gradients prepared in resuspension buffer containing the following Suc concentrations (w/v): from bottom to top, 200 μL of 55% Suc, followed by 450 μL of each 50%, 45%, 40%, 35%, 30%, 25%, and 20% Suc. Gradients were subsequently centrifuged in a bucket rotor at 4°C for 20 h at 100,000g. After centrifugation, gradients were collected in fractions of 200 μL.

Immunoblot Analysis

Total protein was extracted from leaves using 10 volumes (v/w) of protein extraction buffer containing 50 mM Tris-HCl (pH 8.0), 12% (w/v) Suc, 2% (w/v) lithium lauryl sulfate, and 1.5% (w/v) dithiothreitol. The protein concentration of samples was determined using a Rc-Dc protein assay kit (BioRad) with bovine serum albumin (Sigma Chemical) as a protein standard. Before SDS-PAGE separation, all samples were mixed with an equal volume of 2× urea buffer containing 10 mM Tris-HCl (pH 8.0), 10% (w/v) Suc, 2% (w/v) SDS, 1 mM EDTA, 4 mM dithiothreitol, a small amount of bromphenol blue, and 10 M urea and were electrophoresed on a 14% (w/v) polyacrylamide gel and electroblotted to polyvinylidene difluoride membranes. For immunoblots with leaf samples (Supplemental Fig. S1), samples were loaded based on the same weight of fresh leaves. For immunoblots with the subfractions of cells (Fig. 3B), the following amounts of proteins were loaded: membrane and soluble fractions, 2 μg of protein; leaf and chloroplast samples, 12 μg of protein; and vacuole samples, 4 μg of protein. For immunoblots with membrane fractions (Fig. 3C; Supplemental Fig. S2), the same volume of each fraction was loaded on a 14% polyacrylamide gel. CLH1 was detected using anti-CLH1 antiserum raised in rabbits against recombinant Arabidopsis CLH1 expressed in *Escherichia coli*. The following commercial polyclonal antibodies were used in addition: BiP2 (Agrisera) for ER, H$^+$-ATPase (Agrisera) for plasma membrane, V-PPase (CosmoBio, Inc.) for tonoplast, and Lhcb1 (Agrisera) for chloroplasts. Thylakoid membrane abundance was estimated by chlorophyll measurement using HPLC (Zapata et al., 2000).

Analysis of Estradiol-Inducible PPH$_{TP}$-CLH1-Expressing Plants

For estradiol induction, 2 μM 17-β-estradiol was applied as described (Brand et al., 2006) to leaves of plants grown for 7 weeks under short-day conditions. Leaf samples collected after 0, 6, and 9 h of treatment in the dark were used for immunoblot analysis (see above) with antibodies against the HA-tag and for quantification of chlorophyllide a by HPLC (Langmeier et al., 1993). For determination of ion leakage as a measure for cell death, treated leaves were exposed to light (150 μmol m^{-2} s^{-1}) for 2 h and ion conductivity was determined as described (Pruzinská et al., 2007).

CLH Assay

For CLH assays, a method described by Tsuchiya et al. (1997) was used with the following modifications. Leaves were homogenized on ice in 10 volumes (v/w) of assay buffer containing 50 mM Tris-HCl and 38 mM octyl glucoside. After extraction, the homogenate was centrifuged at 4°C for 10 min at 10,000g, and the supernatant was subsequently recovered. The pellet was reextracted identically, and the supernatants were pooled. For assays, 375 μL of the pooled supernatants was added to 125 μL of acetone containing chlorophyll a (500 μg mL^{-1}). Reaction mixtures were incubated for 10 min at 37°C. Reactions were stopped by adding 1.5 mL of hexane:acetone (2:1, v/v) and 50 μL of 2 M Tris-HCl (pH 9.0) to completely ionize chlorophyllide. Mixtures were then shaken and centrifuged at 4°C for 5 min at 10,000g for phase

separation. The lower aqueous layer containing chlorophyllide *a* was recovered, and the concentration of chlorophyllide *a* was quantified spectrophotometrically at 667 nm using an absorption coefficient of 76.79 mM^{-1} cm^{-1} (Porra et al., 1989).

For determining CLH1 activity in plant extracts to mimic mechanical wounding, 50 mg of mature leaves from 7-week-old plants grown under short-day conditions was homogenized with 150 μL of Tris-HCl (pH 8.0) using Shake Master with 5-mm stainless beads. Then, leaf mixtures were kept at room temperature (25°C) for 1 h, and pigments were analyzed by HPLC using the method of Zapata et al. (2000).

Leaf-Feeding Experiments

The wild type, *clh1-1*, and the three CLH1-YFP overexpression lines (nos. 5, 13, and 15) were grown on soil under short-day conditions for 7 weeks. For each independent experiment, 12 plants of each line with similar size were kept separately in boxes (38 mm high and 70-mm diameter; Mineron Kasei Co., Ltd.) at 25°C under light/dark cycles (Supplemental Fig. S4). Five freshly hatched *Spodoptera litura* larvae were then reared on each plant, and the growth and survival status of each larva was analyzed after 4, 7, and 11 d. The χ^2 test was employed for each pair of the wild type and *clh1-1* or a *CLH1*-overexpressing line at each time point (Fig. 6A).

Newly hatched silkworm (*Bombyx mori*) larvae were reared on fresh mulberry (*Morus alba*) leaves at 25°C with a photoperiod of 16 h of light/8 h of dark. After 26 d, for each condition in each independent experiment, three larvae were sacrificed to analyze the pigment compositions in the midgut. The midgut contents (food remains in the midgut) were isolated from the tissue by tweezers. Remaining midgut contents were removed from the tissue by repeated washing with 1× phosphate-buffered saline solution. Frass was also collected from 26-d-old larvae. The midgut contents, midgut tissue, and frass were ground well with cooled acetone at low temperature using Shake Master with 5-mm stainless beads. The extracted pigments were subsequently analyzed by HPLC as described above.

Feeding of Pigments to *S. litura* Larvae

Pigments were dissolved in dimethylformamide and then mixed with an artificial diet (Insecta LFS, Nosan Corporation). The final concentration of dimethylformamide was adjusted to 0.1% (w/w) for all diets used in the experiments. Pigment concentrations of each diet (described as per gram fresh weight) were as follows: control diet (no pigments), chlorophyll *a* (400 nmol g^{-1}), chlorophyllide *a* (either 200 or 400 nmol g^{-1}), and pheophorbide *a* (400 nmol g^{-1}). Freshly hatched *S. litura* larvae were reared in separate tubes in a growth chamber set at 25°C under light/dark conditions. Each artificial diet, with and without added pigment, was fed to a group of 35 to 40 larvae (Supplemental Fig. S5). The developmental status and survival rates for larvae were evaluated after 11 d. To analyze the difference in the developmental stages of the larvae among treatments, a Kruskal-Wallis test was performed with the numbers of dead larvae and those in each developmental stage defined as ordinal variables (Fig. 6B). The death of the larvae was considered as the variable 0, while developmental stages 1 to 4 were considered as the variables 1 to 4, respectively. Multiple comparison of each treatment was performed by the pairwise Wilcoxon rank sum test with a Benjamini-Hochberg false discovery rate correction. All statistical analyses were conducted using the statistical software package R version 2.15.2 (http://r-project.org). The calculated *P* values are shown in Supplemental Table S2. The survival of pigment-fed larvae was statistically analyzed by the Fischer's exact test.

Supplemental Data

The following supplemental materials are available.

Supplemental Figure S1. Total CLH activity and CLH1 protein abundance increase upon MeJA treatment.

Supplemental Figure S2. Localization of CLH1 in fractionated membranes from leaves after 3 d of dark-induced senescence in the presence of 50 μM MeJA.

Supplemental Figure S3. PPH$_{TP}$-CLH1 lines display a severe cell death phenotype.

Supplemental Figure S4. Plant-feeding experiments with freshly hatched *S. litura* larvae.

Supplemental Figure S5. Images of *S. litura* larvae fed with purified pigments for 11 d.

Supplemental Table S1. Effect of chlorophyll-derived pigments on the development of *S. litura* larvae.

Supplemental Table S2. Statistical assessment of the effects of pigment feeding to *S. litura* larvae.

LITERATURE CITED

Abe H, Tateishi K, Seo S, Kugimiya S, Hirai MY, Sawada Y, Murata Y, Yara K, Shimoda T, Kobayashi M (2013) Disarming the jasmonate-dependent plant defense makes nonhost Arabidopsis plants accessible to the American serpentine leafminer. Plant Physiol **163:** 1242–1253

Ayres MP, Clausen TP, MacLean SFJ, Redman AM, Reichardt PB (1997) Diversity of structure and antiherbivore activity in condensed tannins. Ecology **78:** 1696–1712

Azoulay Shemer T, Harpaz-Saad S, Belausov E, Lovat N, Krokhin O, Spicer V, Standing KG, Goldschmidt EE, Eyal Y (2008) Citrus chlorophyllase dynamics at ethylene-induced fruit color-break: a study of chlorophyllase expression, posttranslational processing kinetics, and in situ intracellular localization. Plant Physiol **148:** 108–118

Azoulay-Shemer T, Harpaz-Saad S, Cohen-Peer R, Mett A, Spicer V, Lovat N, Krokhin O, Brand A, Gidoni D, Standing KG, et al (2011) Dual N- and C-terminal processing of citrus chlorophyllase precursor within the plastid membranes leads to the mature enzyme. Plant Cell Physiol **52:** 70–83

Badgaa A, Jia A, Ploss K, Boland W (2014) Chlorophyll degradation in the gut of generalist and specialist lepidopteran caterpillars. J Chem Ecol **40:** 1232–1240

Bekaert M, Edger PP, Hudson CM, Pires JC, Conant GC (2012) Metabolic and evolutionary costs of herbivory defense: systems biology of glucosinolate synthesis. New Phytol **196:** 596–605

Bernays EA, Woodhead S (1982) Plant phenols utilized as nutrients by a phytophagous insect. Science **216:** 201–203

Bones AM, Rossiter JT (1996) The myrosinase-glucosinolate system, its organisation and biochemistry. Physiol Plant **97:** 194–208

Brand L, Hörler M, Nüesch E, Vassalli S, Barrell P, Yang W, Jefferson RA, Grossniklaus U, Curtis MD (2006) A versatile and reliable two-component system for tissue-specific gene induction in Arabidopsis. Plant Physiol **141:** 1194–1204

Clough SJ, Bent AF (1998) Floral dip: a simplified method for *Agrobacterium*-mediated transformation of *Arabidopsis thaliana*. Plant J **16:** 735–743

Cutler SR, Ehrhardt DW, Griffitts JS, Somerville CR (2000) Random GFP: cDNA fusions enable visualization of subcellular structures in cells of Arabidopsis at a high frequency. Proc Natl Acad Sci USA **97:** 3718–3723

Earley KW, Haag JR, Pontes O, Opper K, Juehne T, Song K, Pikaard CS (2006) Gateway-compatible vectors for plant functional genomics and proteomics. Plant J **45:** 616–629

Farmer EE, Dubugnon L (2009) Detritivorous crustaceans become herbivores on jasmonate-deficient plants. Proc Natl Acad Sci USA **106:** 935–940

Golovina GV, Rychkov GN, Ol'shevskaya VA, Zaitsev AV, Kalinin VN, Kuzmin VA, Shtil AA (2013) Differential binding preference of methylpheophorbide *a* and its diboronated derivatives to albumin and low density lipoproteins. Anticancer Agents Med Chem **13:** 639–646

Hayashiya K (1978) Red fluorescent protein in the digestive juice of the silkworm larvae fed on host-plant mulberry leaves. Entomol Exp Appl **24:** 428–436

Hirashima M, Tanaka R, Tanaka A (2009) Light-independent cell death induced by accumulation of pheophorbide *a* in *Arabidopsis thaliana*. Plant Cell Physiol **50:** 719–729

Hu X, Tanaka A, Tanaka R (2013) Simple extraction methods that prevent the artifactual conversion of chlorophyll to chlorophyllide during pigment isolation from leaf samples. Plant Methods **9:** 19

Jonker JW, Buitelaar M, Wagenaar E, Van Der Valk MA, Scheffer GL, Scheper RJ, Plösch T, Kuipers F, Elferink RPJO, Rosing H, et al (2002) The breast cancer resistance protein protects against a major chlorophyll-derived dietary phototoxin and protoporphyria. Proc Natl Acad Sci USA 99: 15649–15654

Kariola T, Brader G, Li J, Palva ET (2005) Chlorophyllase 1, a damage control enzyme, affects the balance between defense pathways in plants. Plant Cell 17: 282–294

Kraatz M, Whitehead TR, Cotta MA, Berhow MA, Rasmussen MA (2014) Effects of chlorophyll-derived efflux pump inhibitor pheophorbide a and pyropheophorbide a on growth and macrolide antibiotic resistance of indicator and anaerobic swine manure bacteria. Int J Antibiot 2014: 1–14

Kruse E, Mock HP, Grimm B (1995) Coproporphyrinogen III oxidase from barley and tobacco—sequence analysis and initial expression studies. Planta 196: 796–803

Langmeier M, Ginsburg S, Matile P (1993) Chlorophyll breakdown in senescent leaves: demonstration of Mg-dechelatase activity. Physiol Plant 89: 347–353

Mauchamp B, Royer C, Garel A, Jalabert A, Da Rocha M, Grenier AM, Labas V, Vinh J, Mita K, Kadono K, et al (2006) Polycalin (chlorophyllid A binding protein): a novel, very large fluorescent lipocalin from the midgut of the domestic silkworm Bombyx mori L. Insect Biochem Mol Biol 36: 623–633

Mauricio R (1998) Costs of resistance to natural enemies in field populations of the annual plant Arabidopsis thaliana. Am Nat 151: 20–28

McFeeters RF, Chichester CO, Whitaker JR (1971) Purification and properties of chlorophyllase from Ailanthus altissima (tree-of-heaven). Plant Physiol 47: 609–618

Meskauskiene R, Nater M, Goslings D, Kessler F, op den Camp R, Apel K (2001) FLU: a negative regulator of chlorophyll biosynthesis in Arabidopsis thaliana. Proc Natl Acad Sci USA 98: 12826–12831

Miller YI, Shaklai N (1999) Kinetics of hemin distribution in plasma reveals its role in lipoprotein oxidation. Biochim Biophys Acta 1454: 153–164

Mithöfer A, Boland W (2012) Plant defense against herbivores: chemical aspects. Annu Rev Plant Biol 63: 431–450

Morant AV, Jørgensen K, Jørgensen C, Paquette SM, Sánchez-Pérez R, Møller BL, Bak S (2008) β-Glucosidases as detonators of plant chemical defense. Phytochemistry 69: 1795–1813

Müller AH, Gough SP, Bollivar DW, Meldal M, Willows RD, Hansson M (2011) Methods for the preparation of chlorophyllide a: an intermediate of the chlorophyll biosynthetic pathway. Anal Biochem 419: 271–276

Oka T, Saito F, Shimma Y, Yoko-o T, Nomura Y, Matsuoka K, Jigami Y (2010) Characterization of endoplasmic reticulum-localized UDP-D-galactose: hydroxyproline O-galactosyltransferase using synthetic peptide substrates in Arabidopsis. Plant Physiol 152: 332–340

Pandian GN, Ishikawa T, Togashi M, Shitomi Y, Haginoya K, Yamamoto S, Nishiumi T, Hori H (2008) Bombyx mori midgut membrane protein P252, which binds to Bacillus thuringiensis Cry1A, is a chlorophyllide-binding protein, and the resulting complex has antimicrobial activity. Appl Environ Microbiol 74: 1324–1331

Park YJ, Kim WS, Ko SH, Lim DS, Lee HJ, Lee WY, Lee DW (2003) Separation and characterization of chlorophyll degradation products in silkworm using HPLC-UV-APCI-MS. J Liquid Chromatogr Relat Technol 26: 3183–3197

Porra RJ, Thompson WA, Kriedemann PE (1989) Determination of accurate extinction coefficients and simultaneous equations for assaying chlorophylls a and b extracted with four different solvents: verification of the concentration of chlorophyll standards by atomic absorption spectroscopy. Biochim Biophys Acta 975: 384–394

Pruzinská A, Anders I, Aubry S, Schenk N, Tapernoux-Lüthi E, Müller T, Kräutler B, Hörtensteiner S (2007) In vivo participation of red chlorophyll catabolite reductase in chlorophyll breakdown. Plant Cell 19: 369–387

Robert S, Zouhar J, Carter C, Raikhel N (2007) Isolation of intact vacuoles from Arabidopsis rosette leaf-derived protoplasts. Nat Protoc 2: 259–262

Salvi D, Rolland N, Joyard J, Ferro M (2008) Purification and proteomic analysis of chloroplasts and their sub-organellar compartments. In D Pflieger, J Rossier, eds, Organelle Proteomics. Humana Press, Totowa, NJ, pp 19–36

Saunders JA, Conn EE (1978) Presence of the cyanogenic glucoside dhurrin in isolated vacuoles from Sorghum. Plant Physiol 61: 154–157

Schelbert S, Aubry S, Burla B, Agne B, Kessler F, Krupinska K, Hörtensteiner S (2009) Pheophytin pheophorbide hydrolase (pheophytinase) is involved in chlorophyll breakdown during leaf senescence in Arabidopsis. Plant Cell 21: 767–785

Schenk N, Schelbert S, Kanwischer M, Goldschmidt EE, Dörmann P, Hörtensteiner S (2007) The chlorophyllases AtCLH1 and AtCLH2 are not essential for senescence-related chlorophyll breakdown in Arabidopsis thaliana. FEBS Lett 581: 5517–5525

Song HY, Rho MC, Lee SW, Kwon OE, Chang YD, Lee HS, Kim YK (2002) Isolation of Acyl-CoA:cholesterol acyltransferase inhibitor from Persicaria vulgaris. Planta Med 68: 845–847

Tapper BA, Lohrey E, Hove EL, Allison RM (1975) Photosensitivity from chlorophyll-derived pigments. J Sci Food Agric 26: 277–284

Thayer SS, Conn EE (1981) Subcellular localization of dhurrin β-glucosidase and hydroxynitrile lyase in the mesophyll cells of Sorghum leaf blades. Plant Physiol 67: 617–622

Tsuchiya T, Ohta H, Masuda T, Mikami B, Kita N, Shioi Y, Takamiya K (1997) Purification and characterization of two isozymes of chlorophyllase from mature leaves of Chenopodium album. Plant Cell Physiol 38: 1026–1031

Tsuchiya T, Ohta H, Okawa K, Iwamatsu A, Shimada H, Masuda T, Takamiya K (1999) Cloning of chlorophyllase, the key enzyme in chlorophyll degradation: finding of a lipase motif and the induction by methyl jasmonate. Proc Natl Acad Sci USA 96: 15362–15367

Vencl FV, Gómez NE, Ploss K, Boland W (2009) The chlorophyll catabolite, pheophorbide a, confers predation resistance in a larval tortoise beetle shield defense. J Chem Ecol 35: 281–288

Vetter J (2000) Plant cyanogenic glycosides. Toxicon 38: 11–36

War AR, Paulraj MG, Ahmad T, Buhroo AA, Hussain B, Ignacimuthu S, Sharma HC (2012) Mechanisms of plant defense against insect herbivores. Plant Signal Behav 7: 1306–1320

Willstätter R, Stoll A (1913) Die wirkungen der chlorophyllase. In R Willstätter, A Stoll, eds, Untersuchungen über Chlorophyll. Springer, Berlin, pp 172–187

Windram O, Madhou P, McHattie S, Hill C, Hickman R, Cooke E, Jenkins DJ, Penfold CA, Baxter L, Breeze E, et al (2012) Arabidopsis defense against Botrytis cinerea: chronology and regulation deciphered by high-resolution temporal transcriptomic analysis. Plant Cell 24: 3530–3557

Wulfetange K, Lomin SN, Romanov GA, Stolz A, Heyl A, Schmülling T (2011) The cytokinin receptors of Arabidopsis are located mainly to the endoplasmic reticulum. Plant Physiol 156: 1808–1818

Zapata M, Rodríguez F, Garrido JL (2000) Separation of chlorophylls and carotenoids from marine phytoplankton, a new HPLC method using a reversed phase C_8 column and pyridine-containing mobile phases. Mar Ecol Prog Ser 195: 29–45